In-situ environmental radiation background measurement in the second phase of CJPL

Peng Zhang[1], Zhi Zeng[1], Jianping Cheng[1,2], Hao Ma[1,*]

08/25/2025

[1]Key Laboratory of Particle and Radiation Imaging (Ministry of Education) and Department of Engineering Physics, Tsinghua University, Beijing 100084, China

[2]Beijing Normal University, Beijing 100875, China

*Corresponding author: mahao@tsinghua.edu.cn

The XIX International Conference on Topics in Astroparticle and Underground Physics (TAUP2025)

Contents

Introduction: CJPL-II

- Deepest lab with 2400 m rock overburden → Low cosmic-ray muon flux and radiation background
- Largest underground lab (>300,000 m^3) + Direct access by road tunnels → Convenient and comfortable working env[1]

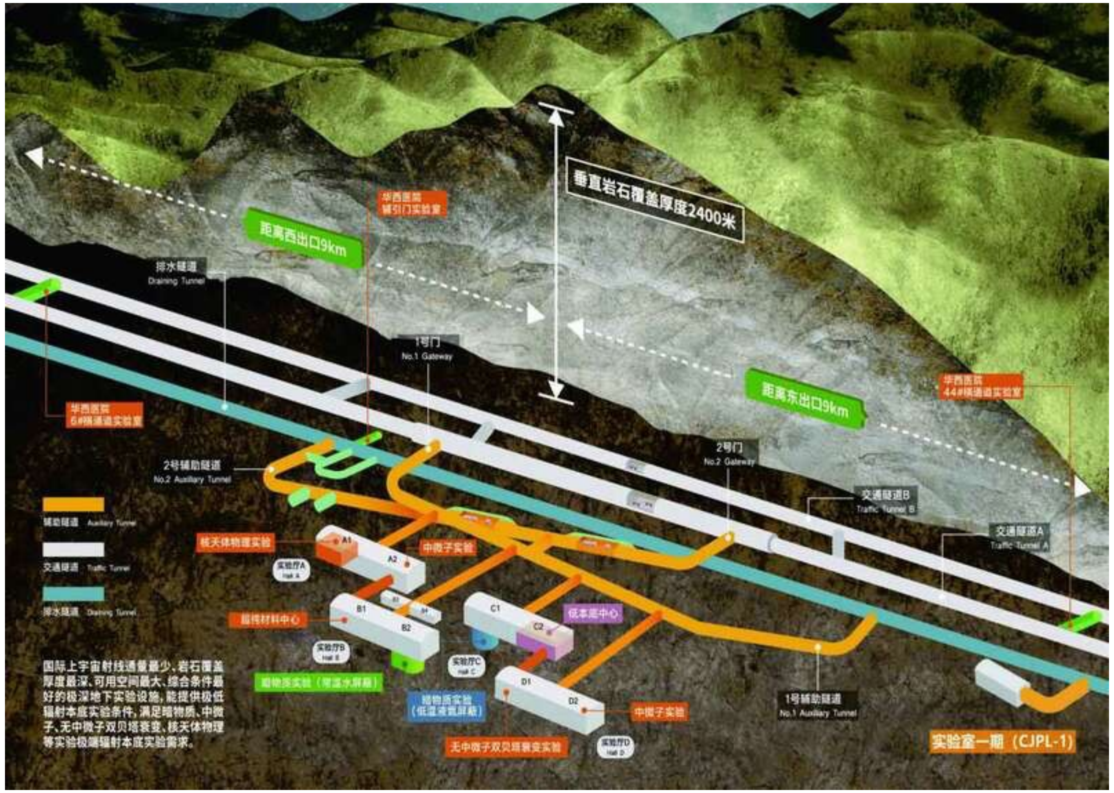

Illustration of the CJPL-II

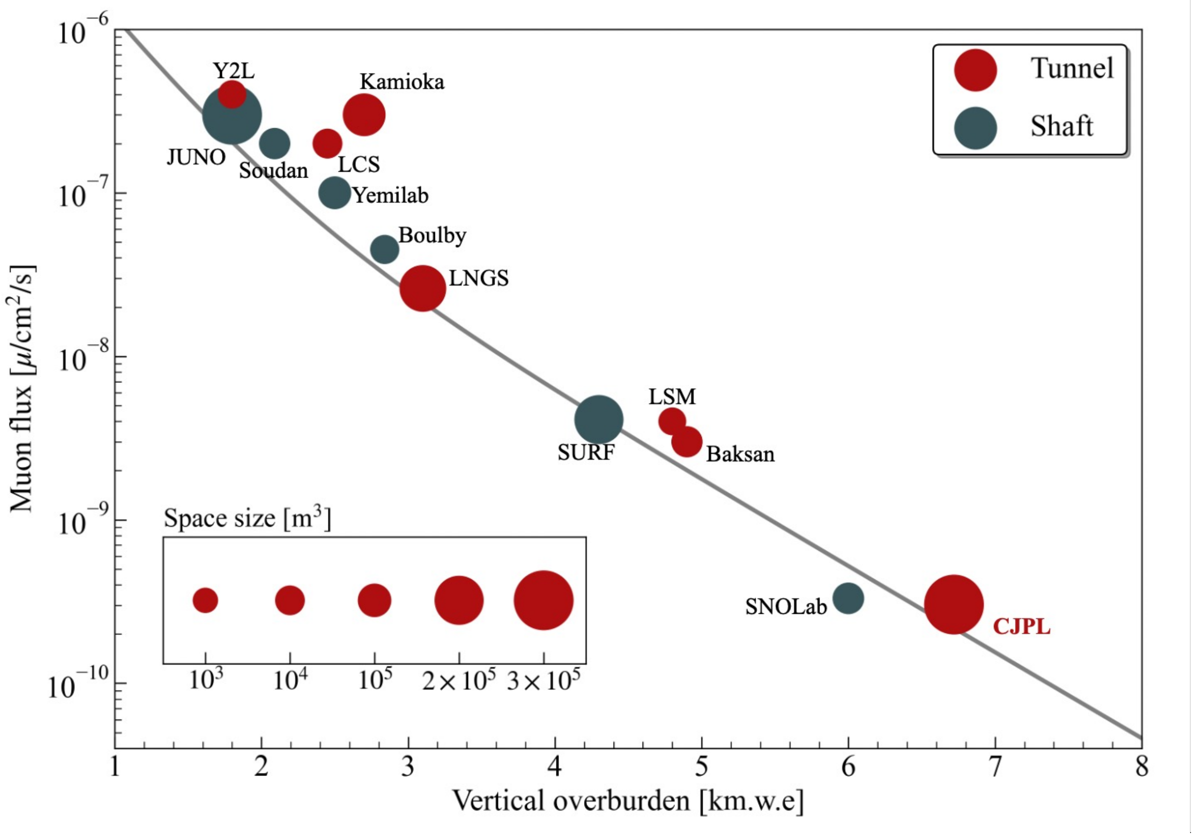

Parameters of the major underground labs

[1] J. Cheng, et al., Annu. Rev. Nucl. Part. Sci. 67 (2017) 231–251

Introduction: CJPL-II Environmental radiation sources

- Cosmic-ray muons → **residual muons**, muon-induced radioactivity (**neutrons**, cosmogenic nuclides)
- Radioactivity from bedrock and building materials:
  - ^{238}U series, ^{232}Th series, ^{40}K → **gamma-rays**, beta, alpha
  - ^{238}U， ^{235}U， ^{232}Th → **neutrons** (spontaneous fission and (α, n) reactions)
- Radioactivity from air: Radon → **gamma-rays**, beta, alpha

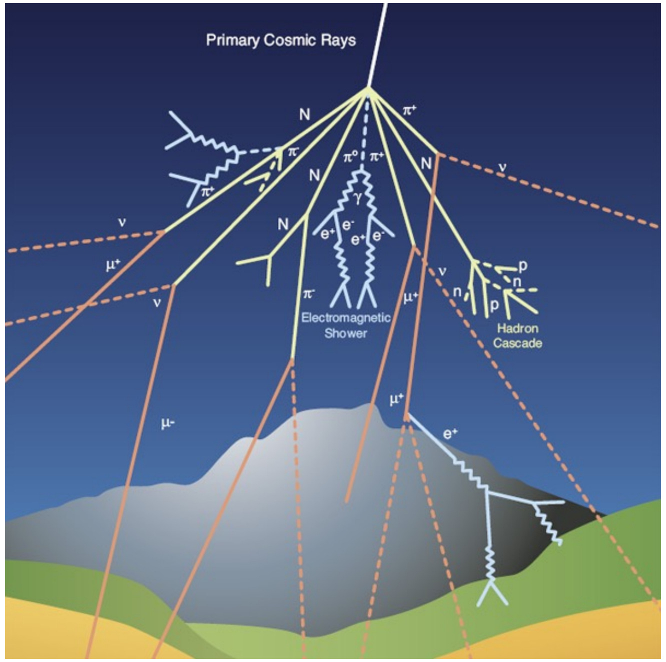

Illustration of the cosmic-ray muons

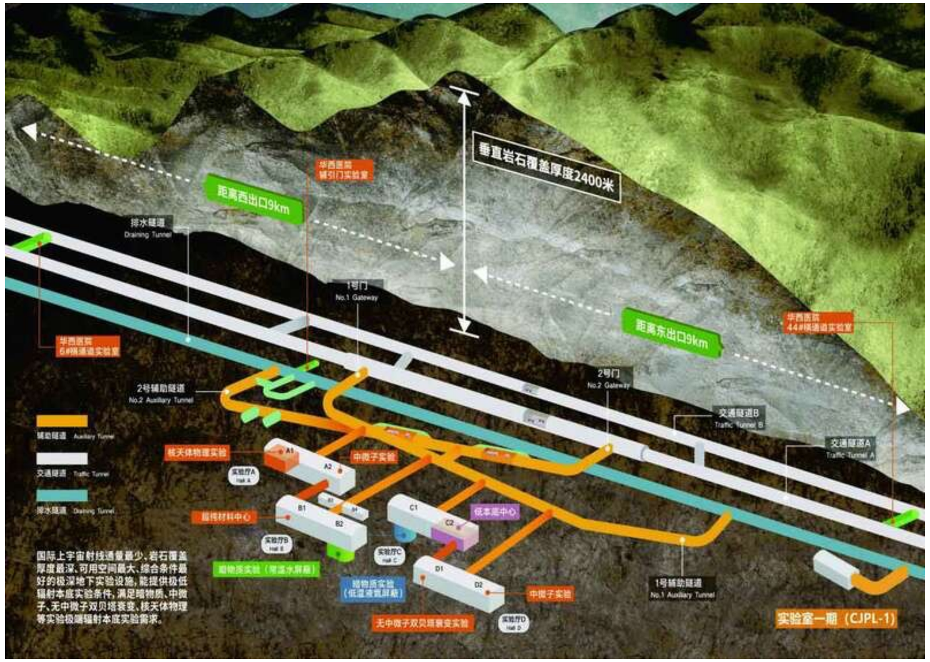

CJPL-II layout[1]

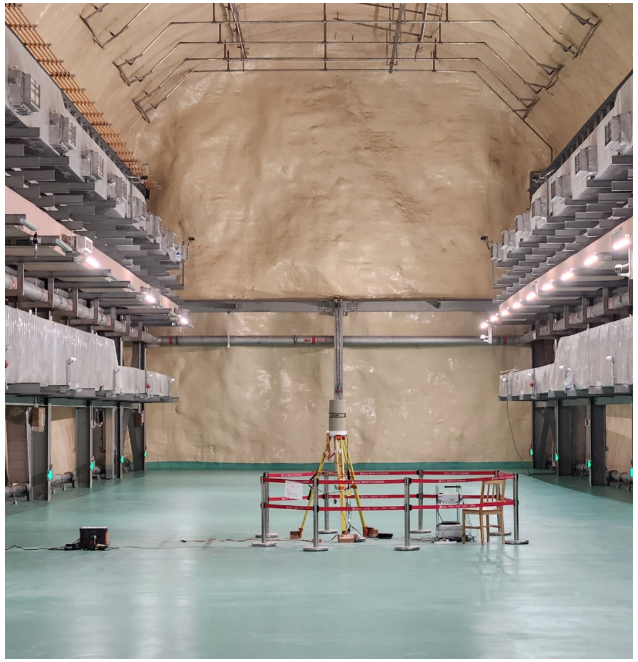

CJPL-II experimental hall A1

Cosmic-ray muons

- Measurement: 2016-2020 at CJPL-II Hall C2
  - Detector: a two-group three-layer plastic scintillator telescope system

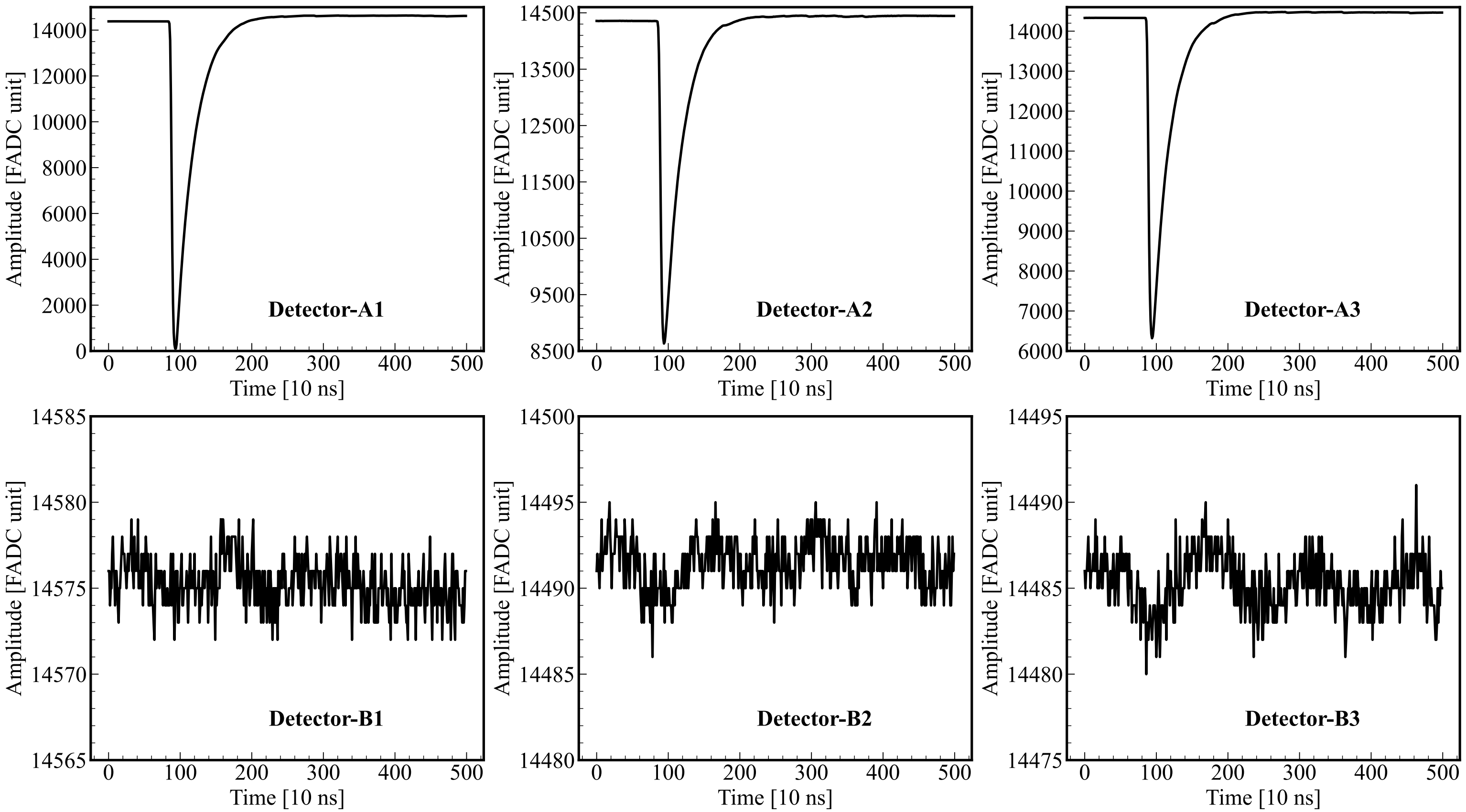

Detector signals when a muon passed three detectors of group A

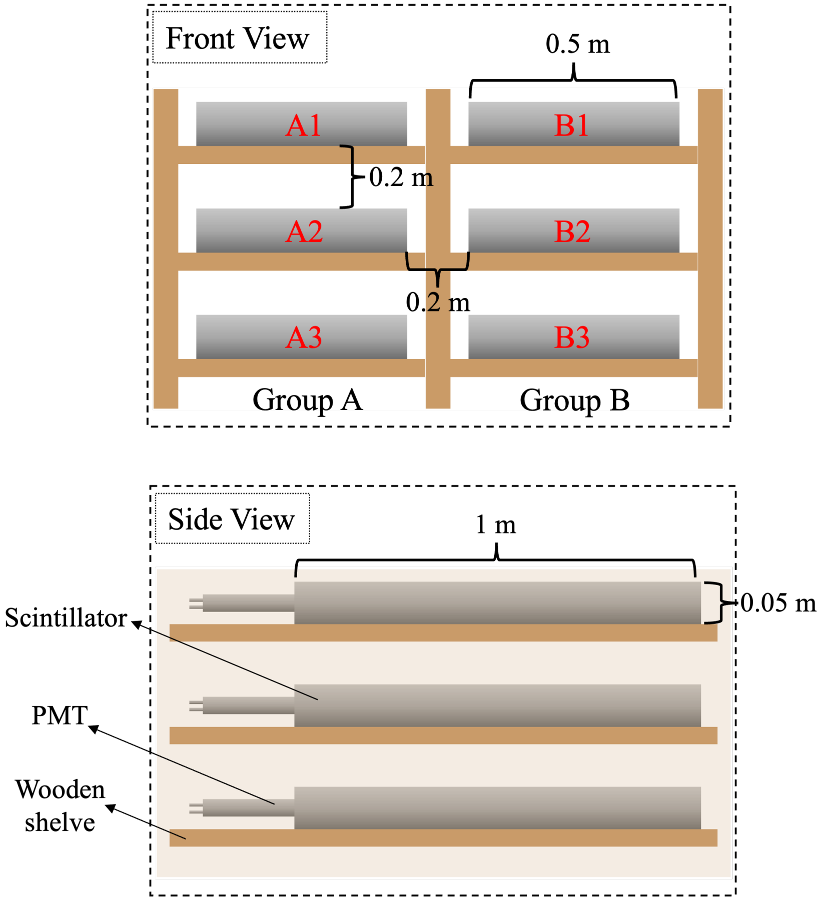

Schematic of the muon telescope system

[2] P. Zhang, et al., Astroparticle Physics, 172 (2025) 103147

Cosmic-ray muons

- Data analysis: 1) data quality check 2) rise/fall time restrain 3) amplitude restrain 4) triple coincidence
- Measured muon flux (w/o efficiency correction): $\phi_m = (1.70 \pm 0.13(\mathrm{stat})) \times 10^{-10}\ \mathrm{cm}^{-2}\mathrm{s}^{-1}$

Detector group	Live time (days)	Number of muon events	Muon flux ($\mathrm{cm}^{-2}\mathrm{s}^{-1}$)
A	1098	85	$(1.80 \pm 0.19) \times 10^{-10}$
B	1098	76	$(1.60 \pm 0.18) \times 10^{-10}$
Total	1098	161	$(1.70 \pm 0.13) \times 10^{-10}$

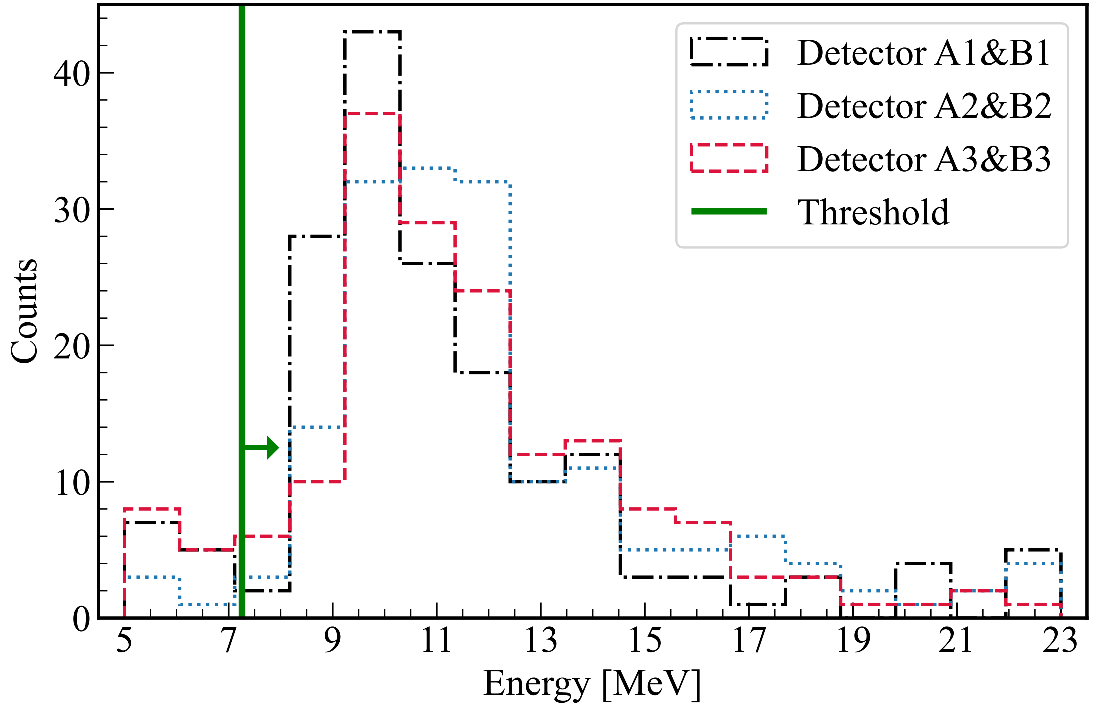

Energy spectra of triple coincidence signals

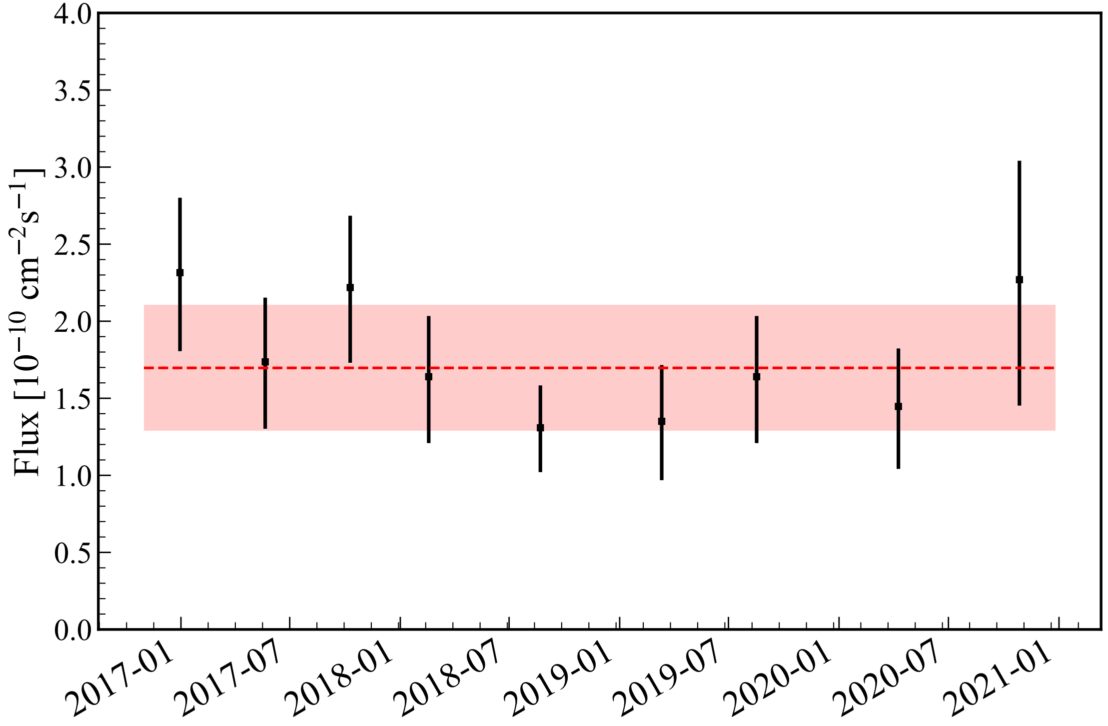

Measured muon flux over time (w/o efficiency correction)

[2] P. Zhang, et al., Astroparticle Physics, 172 (2025) 103147

Cosmic-ray muons

- Efficiency calculation:
  - Transportation in the Mountain: MUSIC
    - Ground muon pdf: modified Gaisser Formula
    - Rock depth to travel through
  - Detection in the lab: Geant4
- Overall efficiency: $\varepsilon = (0.562 \pm 0.005(\text{stat}) \pm 0.033(\text{sys}))$

<u>Muon flux at CJPL-II:</u>

$$\phi = (3.03 \pm 0.24(\text{stat}) \pm 0.18(\text{sys}))\times10^{-10}\ \text{cm}^{-2}\text{s}^{-1}$$

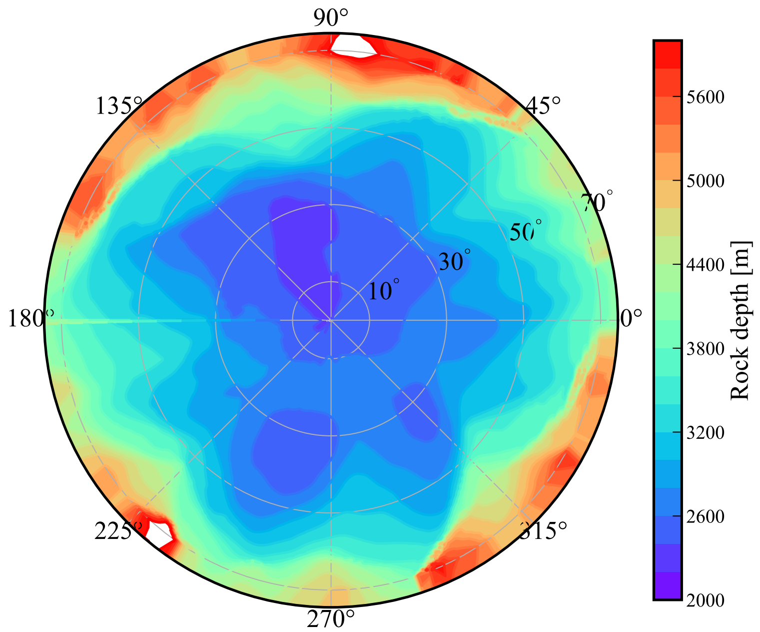

Rock depth angular pdf

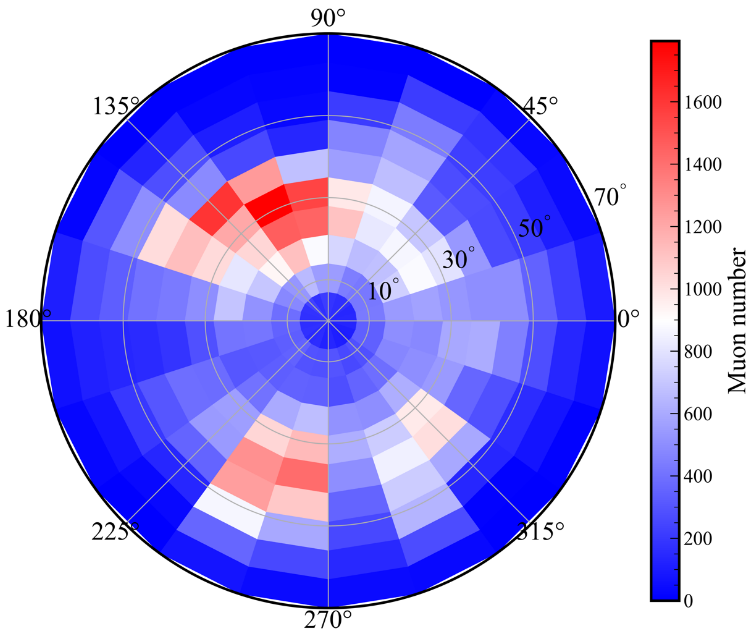

Underground muon angular pdf

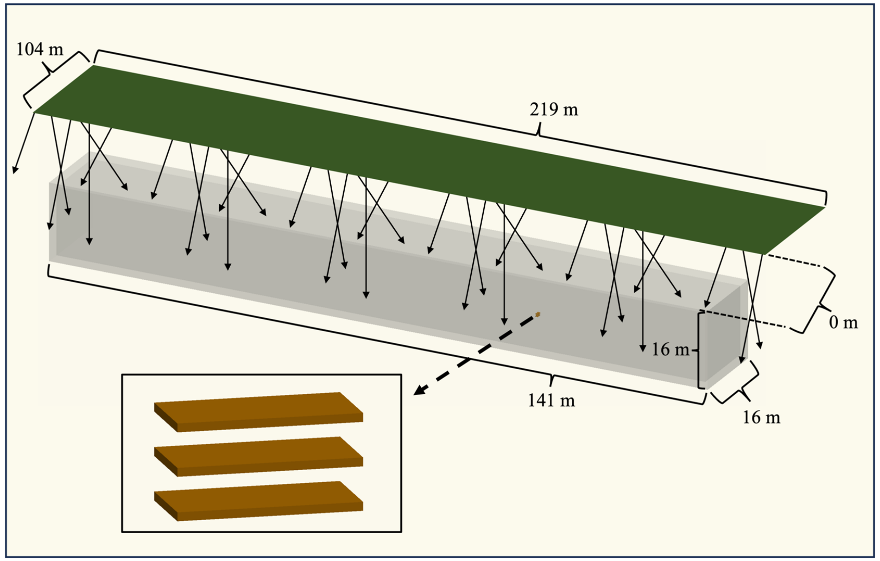

Illustration of the final efficiency simulation

[2] P. Zhang, et al., Astroparticle Physics, 172 (2025) 103147

Radon: Water-Resistant and Radon Suppression layer

- Water-Resistant and Radon Suppression (WRRS) layer [3]
  - Radon exhalation reduced to less than 1% of its initial value: $6.98 \pm 0.33\ \mathrm{mBq \cdot m^{-2} \cdot s^{-1}} \rightarrow < 0.088\ \mathrm{mBq \cdot m^{-2} \cdot s^{-1}}$ [4]

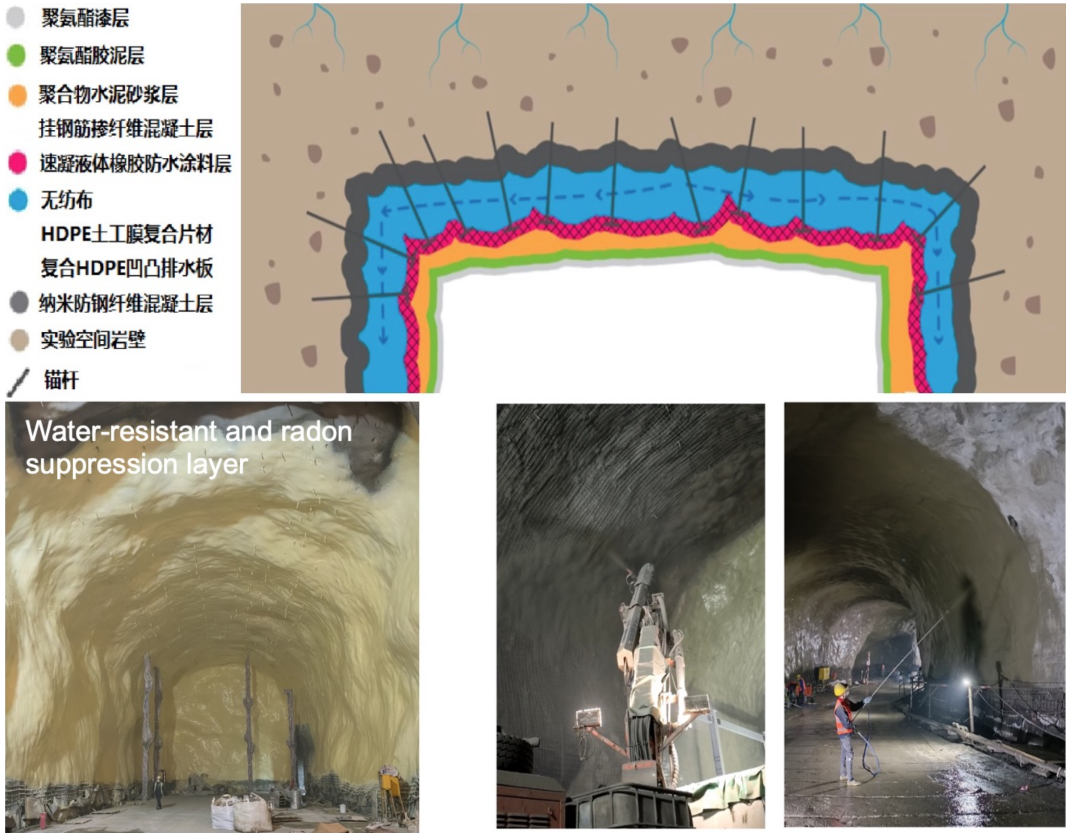

The WRRS layer[4]

Surface radon exhalation rate detector on various surfaces[3]

[3] Pengcheng Xu, Study on the Source and Prediction of Indoor Radon Concentration in Jinping Great Facility, Master thesis, Tsinghua, 2023
[4] Q. Zhang, et al., Sci Sin-Phys Mech Astron, 2025, 55:111018

Radon: Concentration monitoring

- Instrument: AlphaGuard
- Before the WRRS project, the average concentration: 208.0 ± 0.1 Bq/m^3

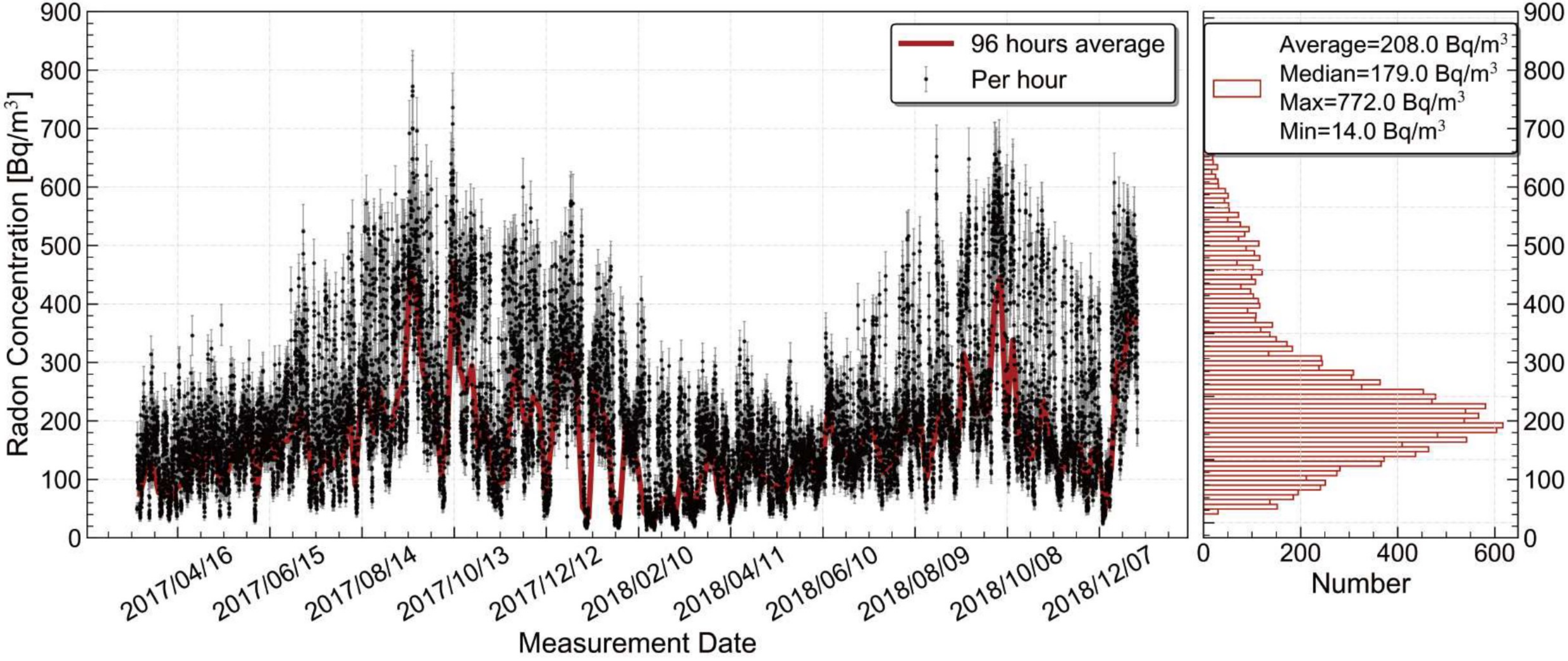

Measurement results of radon concentration in hall C2 before the WRRS project

[4] Q. Zhang, et al., Sci Sin-Phys Mech Astron, 2025, 55:111018

Radon: Concentration monitoring

- Instrument: AlphaGuard
- After the WRRS project and ventilation, the average concentration: 20.3 ± 0.1 Bq/m^3

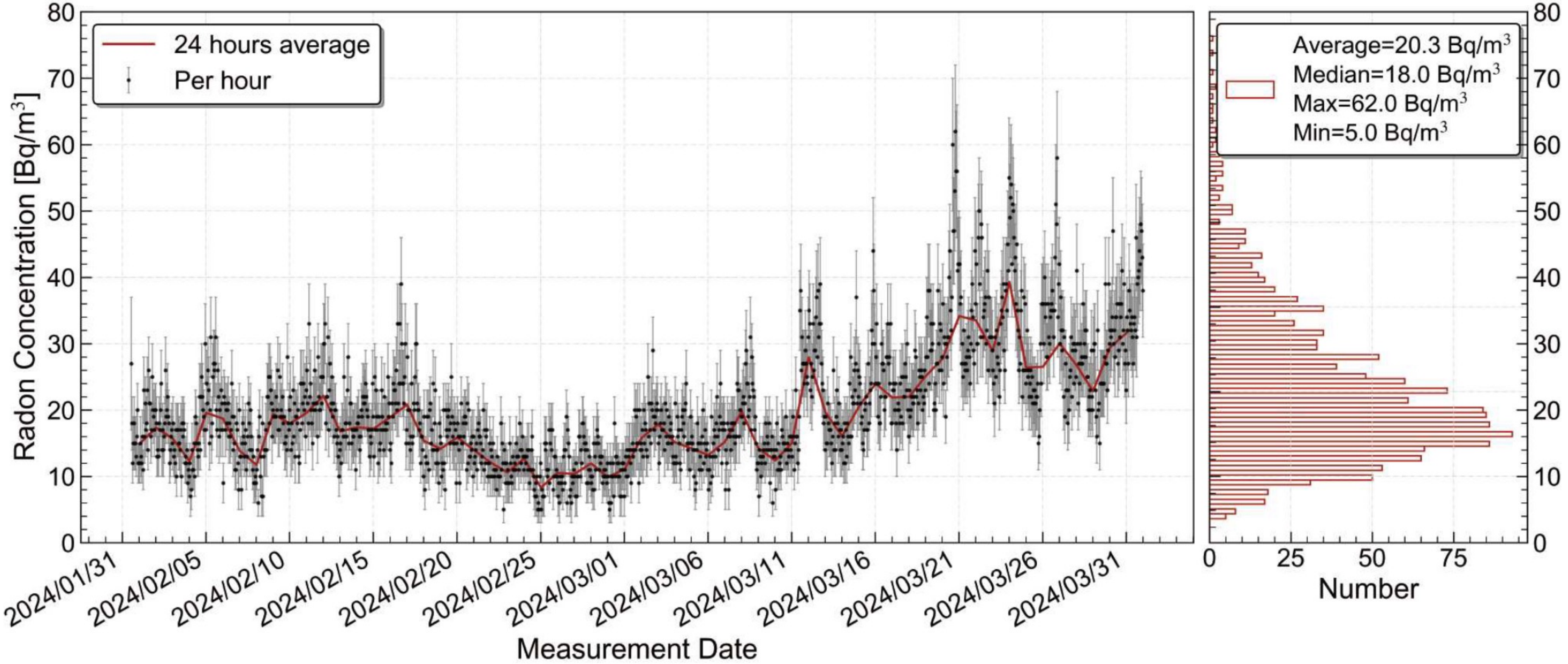

Measurement results of radon concentration in hall A1 After the WRRS project

[4] Q. Zhang, et al., Sci Sin-Phys Mech Astron, 2025, 55:111018

Gamma rays

- 2024, In-situ gamma spectrum measurement (after construction of DURF*):
  - Location: 1) Hall A1 2) connecting tunnel CD

    3) inside and 4) outside the PE chamber in Hall C2
  - Detector HPGe (59.1×58.8 mm): measure the gamma spectrum
  - Detector Alpha Guard: assess the contribution of radon to the spectrum

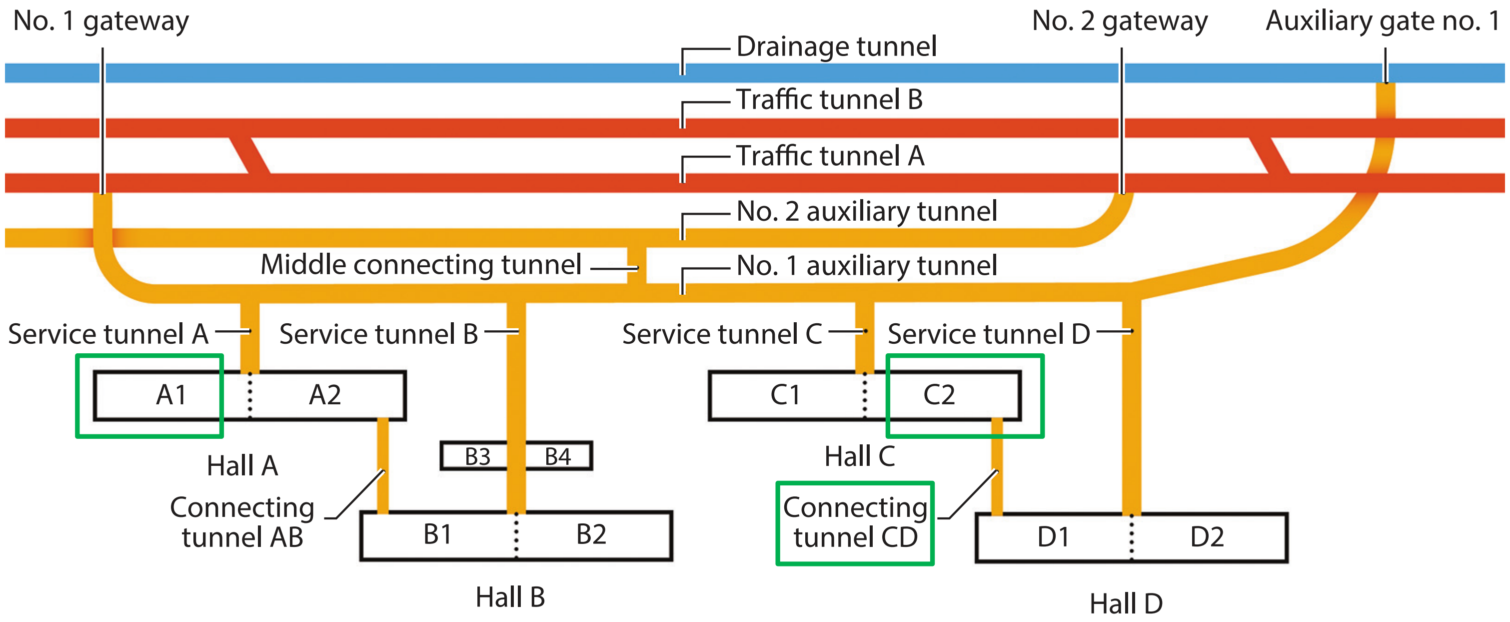

Illustration of the measurement position

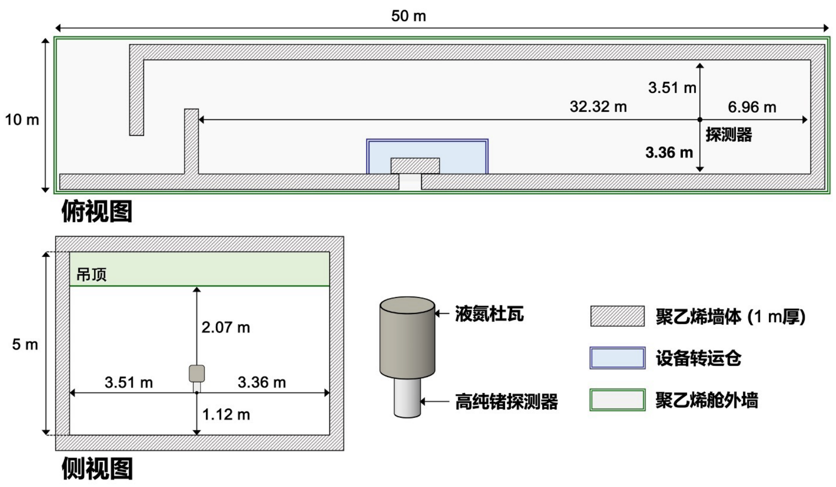

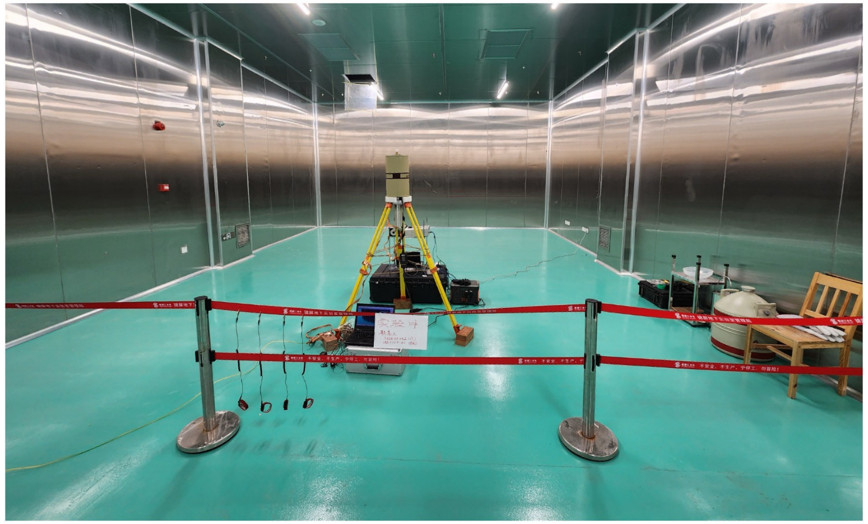

The detector system inside the PE chamber

[5] P. Zhang, et al., Sci Sin-Phys Mech Astron, 2025, 55:111017 | *DURF: **D**eep **U**nderground and ultra-low **R**adiation background **F**acility for frontier physics experiments

Gamma rays

- The detection efficiency of nuclides ^{238}U, ^{232}Th, and ^{40}K in the environmental building materials:

$$R = R_{\mathrm{env}} + R_{\mathrm{Rn}} = K_{\mathrm{env}} \times A_{\mathrm{env}} + K_{\mathrm{Rn}} \times C_{\mathrm{Rn}}$$

env nuclide activity (A_{env}); Radon concentration (C_{Rn})

$$K_{\mathrm{env}}(E) = \rho P(E) \int_{z_{\min}}^{z_{\max}} \int_{y_{\min}}^{y_{\max}} \int_{x_{\min}}^{x_{\max}} f_A(E,\theta) \frac{e^{-\sum_i \mu_i l_i}}{r^2} dxdydz$$

branching ratio ($P(E)$); angular response ($f_A(E,\theta)$)

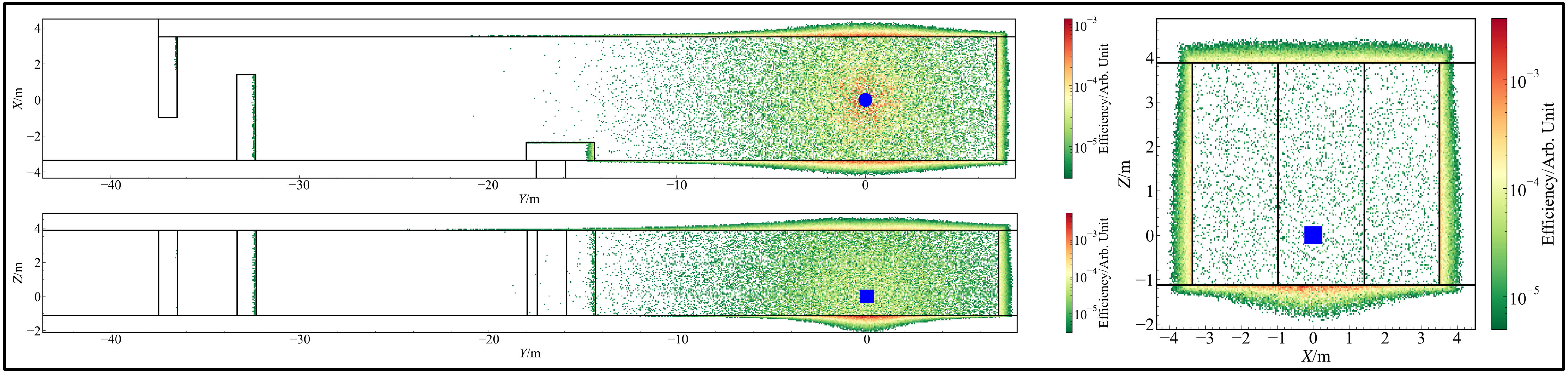

Detection efficiency of nuclides for different positions of the PE walls in Hall C2

[6] P. Zhang, et al., Calculation of nuclide activity conversion factor for in-situ gamma-ray measurement, 2025, accepted by Nuclear Techniques, https://doi.org/10.57760/sciencedb.hjs.00383

Gamma rays

- Artificial radionuclides such as ^{60}Co and ^{137}Cs were not detected in the spectra
- The integral count rate of the gamma spectrum inside the PE chamber of Hall C2 was 31 times lower than that outside
- The environmental gamma background is among the first tier :
  - ^{238}U: 4.69-5.81 Bq/kg, ^{232}Th: 5.57-6.66 Bq/kg, ^{40}K: 127.00-149.44 Bq/kg

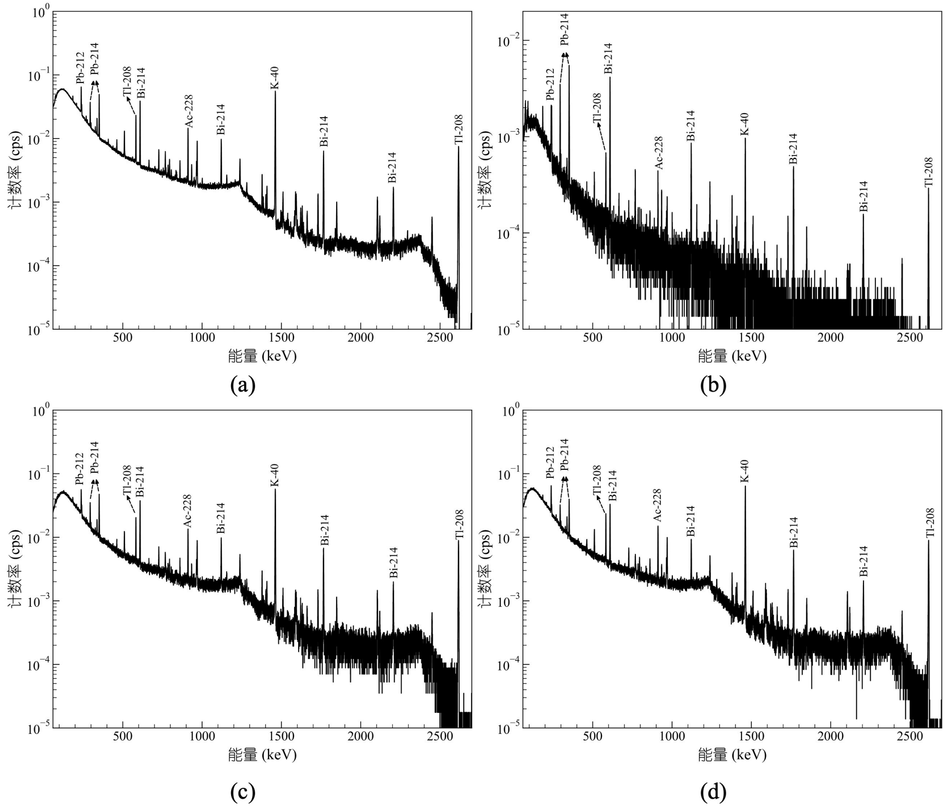

Measured gamma spectra

Underground lab	Detector	Energy range [keV]	Integral count rate [cps]	Radioactivity concentration [Bq/kg]		
				^{238}U	^{232}Th	^{40}K
Gran Sasso[10]	NaI	35-3000	69.5	9.5±0.3	3.7±0.2	70±2
Modane[11]	HPGe	7-2734	79	22.8±0.7	6.7±0.2	91±3
Boulby[9]	HPGe	7-2734	24	7.1±0.2	3.9±0.1	120±2
Sanford[12]	NaI	0-3300	596~1335	29±15	13±3	220±60
SNOLAB[13]	NaI	0-3300	92.5	14.7±0.4	9.7±0.5	232.8±15.8
CJPL-I[19]	HPGe	60-2700	73.4	18.0	7.6	36.7
CJPL-II[15]	HPGe	60-2700	46.8	6.8±1.5	5.4±0.6	81.9±14.4
CJPL-II (This work)						
Hall A1	HPGe	60-2700	77.4	5.81±0.06	6.66±0.03	148.86±1.70
Hall C2 (outside PE chamber)	HPGe	60-2700	69.9	4.69±0.12	6.19±0.04	149.44±1.66
Hall C2 (inside PE chamber)	HPGe	60-2700	2.2	<1.240	<0.217	<2.379
CD connecting channel	HPGe	60-2700	75.2	5.25±0.04	5.57±0.02	127.00±0.78

Summary of the CJPL-II in-situ gamma measurement

[5] P. Zhang, et al., Sci Sin-Phys Mech Astron, 2025, 55:111017 | *DURF: **D**eep **U**nderground and ultra-low **R**adiation background **F**acility for frontier physics experiments

Neutrons

- Measurement: 2016 at CJPL-II, Bonner multi-sphere spectrometer + Unfolding code based on the genetic algorithm
- Validation: ^{252}Cf source (its neutron energy follows the Maxwell-Boltzmann distribution)

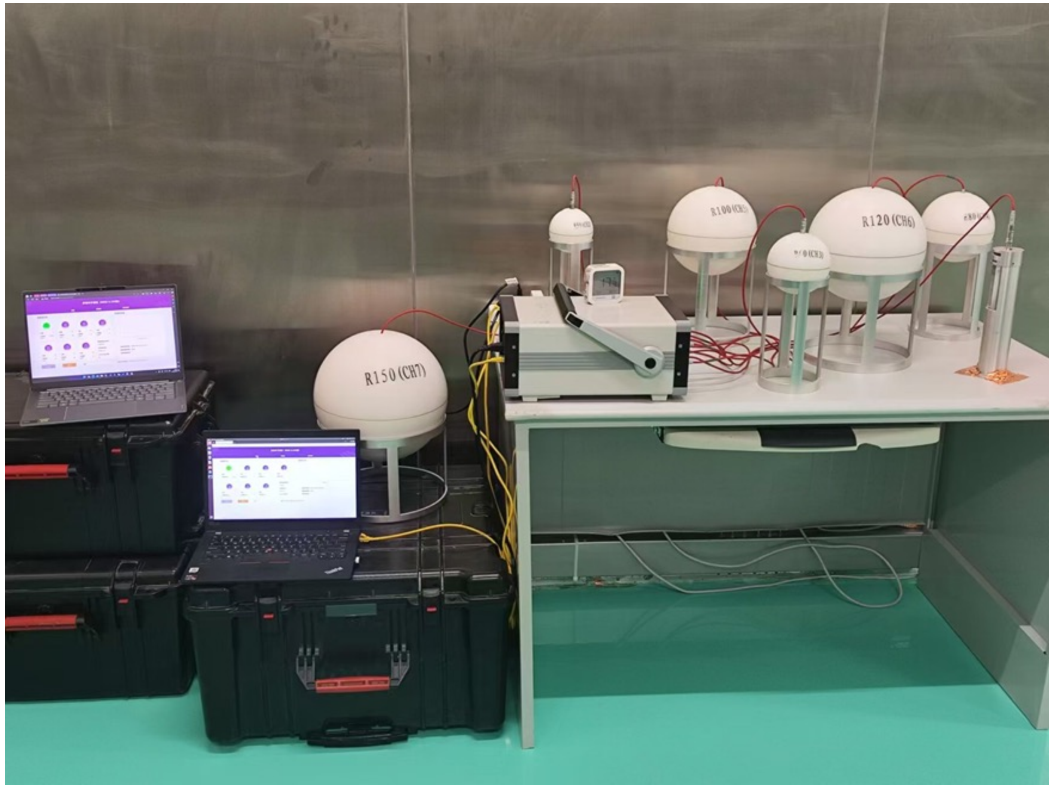

Bonner multi-sphere spectrometer

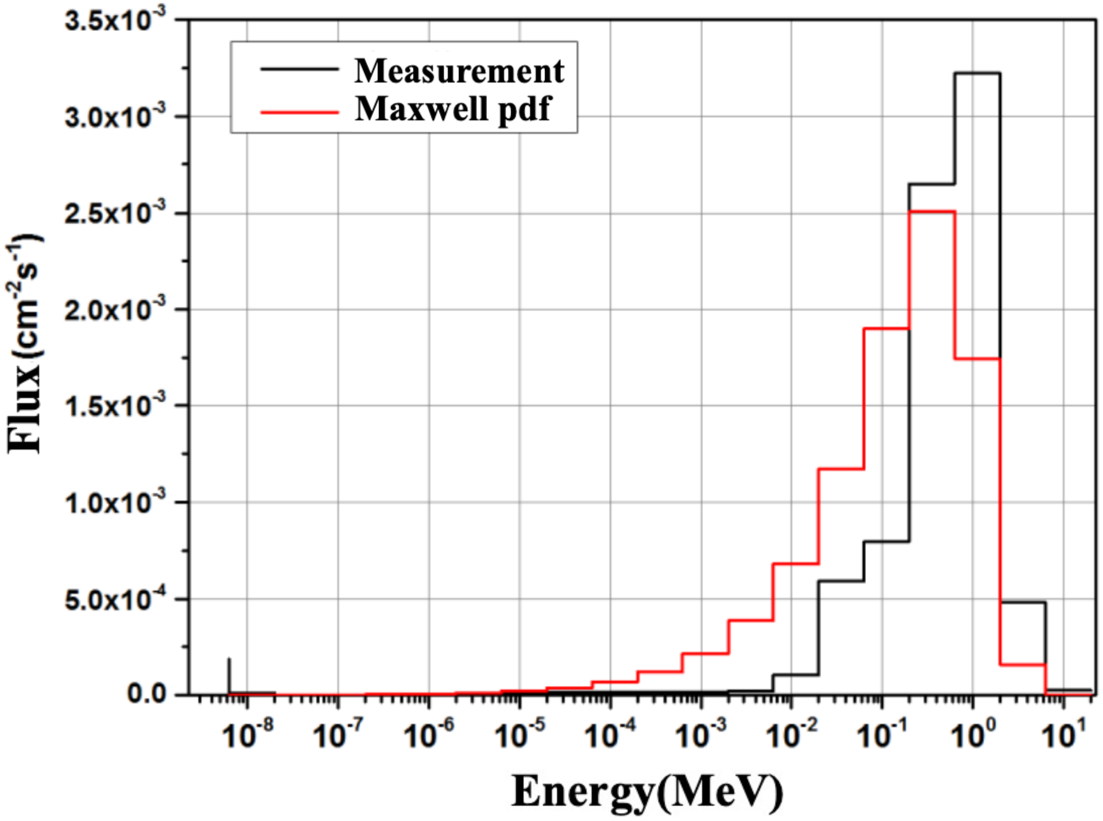

Measured and theoretical spectra

[7] Qingdong Hu, Background Research of Tonne-Scale Germanium Detector for Dark Matter Searches, Doctoral thesis, Tsinghua, 2018 [8] Q. Hu, et al., NIMA, 859 (2017) 37–40

Neutrons

- Results

Fast neutron (1-10 MeV)	Thermal neutron (< 0.5 eV)
$(3.8 \pm 0.6)\times10^{-7}\ \text{cm}^{-2}\text{s}^{-1}$	$(1.1 \pm 0.2)\times10^{-5}\ \text{cm}^{-2}\text{s}^{-1}$

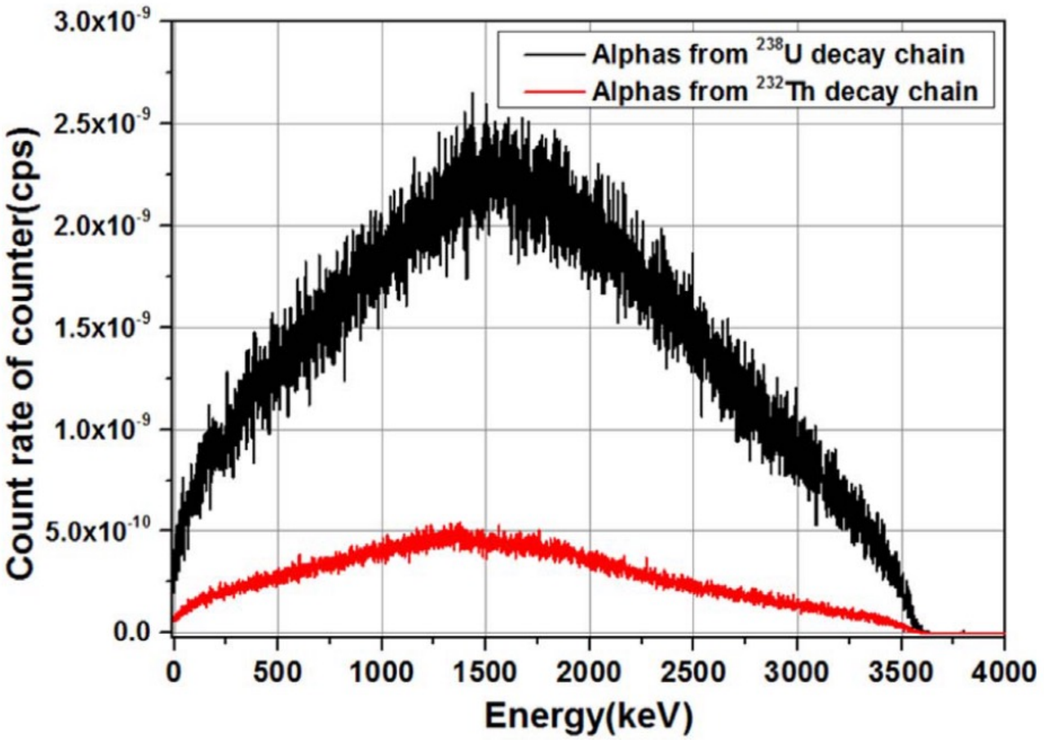

Simulated alpha background spectrum

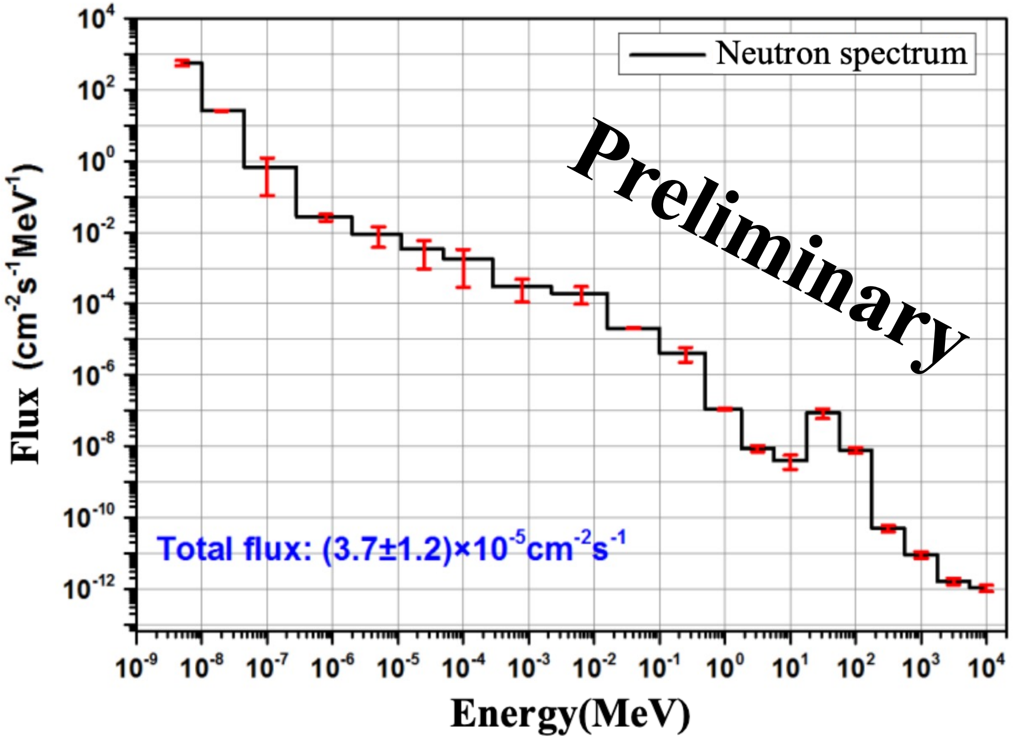

Measured neutron spectrum in CJPL-II

Neutrons

- Neutron flux in CJPL-II is around 10^3 times lower than ground level (2.8×10^{-2} $cm^{-2}s^{-1}$ [12])
- Neutron flux is further reduced a lot in the PE chamber of Hall C2 (fast: ~30 times, thermal: ~20 times)
- Cosmic-ray muon induced neutron (by simulation, total)[13]: $(8.0 \pm 0.8)\times10^{-11}$ $cm^{-2}s^{-1}$

Measurement	Site	Total flux / $cm^{-2}s^{-1}$	Fast neutron / $cm^{-2}s^{-1}$	Thermal neutron / $cm^{-2}s^{-1}$
Bonner Multi-sphere, 2016[7]	CJPL-II, Hall C	$(3.7 \pm 1.2)\times10^{-5}$	$(3.8 \pm 0.6)\times10^{-7}$ (1-10 MeV)	$(1.1 \pm 0.2)\times10^{-5}$ (< 0.5 eV)
^{3}He tube, 2016[9]	CJPL-II, Hall C	\	\	$(9.8 \pm 0.3)\times10^{-6}$
Bonner Multi-sphere, 2016[8]	CJPL-I, Hall A	$(2.7 \pm 1.0)\times10^{-5}$	$(3.6 \pm 2.8)\times10^{-6}$ (> 1 MeV)	$(7.0 \pm 1.8)\times10^{-6}$ (< 0.5 eV)
Liquid scintillator, 2017[11]	CJPL-I, PE chamber	\	$(4.9 \pm 1.0)\times10^{-9}$ (1-10 MeV)	\
Liquid scintillator, 2017[11]	CJPL-I, Hall A	\	$(1.5 \pm 0.1)\times10^{-7}$ (1-10 MeV)	\
^{3}He tube, 2014[10]	CJPL-I, Hall A	\	\	$(4.0 \pm 0.1)\times10^{-6}$
^{3}He tube, 2015[9]	CJPL-I, PE chamber	\	\	$(2.2 \pm 0.2)\times10^{-7}$
^{3}He tube 2017[9]	CJPL-I, PE chamber, inside the CDEX-1B shielding	\	\	$(2.8 \pm 1.2)\times10^{-8}$

[9] Zhaoming Zeng, Research and Application of Low Background Thermal Neutron Detection Technology, Tsinghua, 2017 [10] Z. Zeng, et al., NIMA, 804 (2015) 108–112 [11] Q. Du, et al., NIMA, 889 (2018) 105–112
[12] Sato T, Expacs excel-based program for calculating atmospheric cosmic-ray spectrum, https://phits.jaea.go.jp/expacs/. [13] J. Su, et al., High Power Laser and Particle Beams, 2015, DOI:10.3788/HPLPB20122412.3015

Summary

- The cosmic-ray muon flux in CJPL-II is the lowest worldwide: $(3.03 \pm 0.24(\text{stat}) \pm 0.18(\text{sys}))\times 10^{-10}\ \text{cm}^{-2}\text{s}^{-1}$
- With the Water-Resistant and Radon Suppression project, the Radon exhalation rate was reduced from 6.98 to less than $0.88\ \text{mBq}\cdot\text{m}^{-2}\cdot\text{s}^{-1}$. The Radon concentration was reduced from 208.0 to 20.3 Bq/m^3
- The environmental gamma background is among the first tier:
  - ^{238}U: 4.69-5.81 Bq/kg, ^{232}Th: 5.57-6.66 Bq/kg, ^{40}K: 127.00-149.44 Bq/kg
  - The integral count rate of the gamma spectrum inside the PE chamber of Hall C2 was 31 times lower than that outside
- The underground neutron flux is $(3.7 \pm 1.2)\times 10^{-5}\text{cm}^{-2}\text{s}^{-1}$
  - It is around 10^3 times lower than ground level
  - Neutron flux is further reduced a lot in the PE chamber of Hall C2 (fast: ~30 times, thermal: ~20 times)

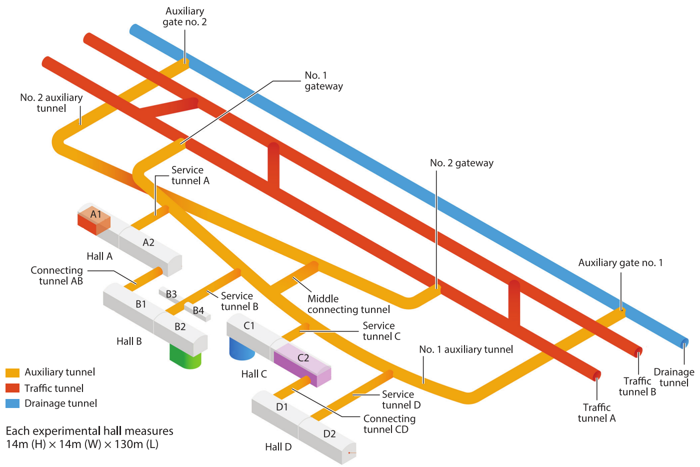

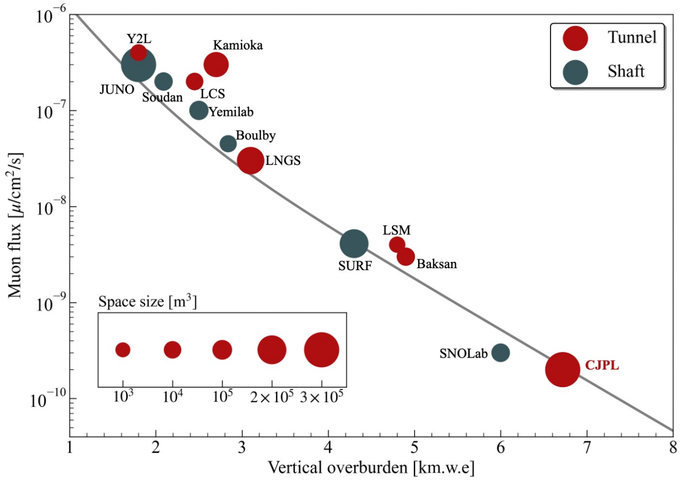

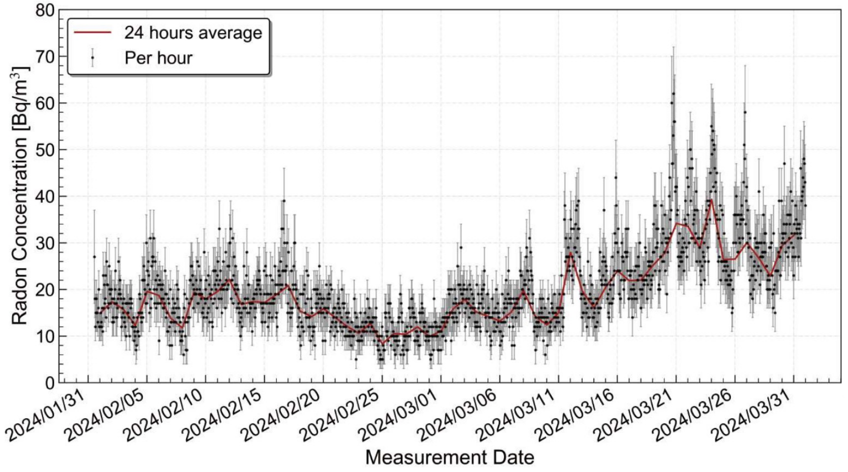

Thanks!

[1] J. Cheng, et al., Annu. Rev. Nucl. Part. Sci. 67 (2017) 231–251
[2] P. Zhang, et al., Astroparticle Physics, 172 (2025) 103147
[3] Pengcheng Xu, Study on the Source and Prediction of Indoor Radon Concentration in Jinping Great Facility, Master thesis, Tsinghua, 2023
[4] Q. Zhang, et al., Sci Sin-Phys Mech Astron, 2025, 55:111018
[5] P. Zhang, et al., Sci Sin-Phys Mech Astron, 2025, 55:111017
[6] P. Zhang, et al., Calculation of nuclide activity conversion factor for in-situ gamma-ray measurement, 2025, accepted by Nuclear Techniques, https://doi.org/10.57760/sciencedb.hjs.00383
[7] Qingdong Hu, Background Research of Tonne-Scale Germanium Detector for Dark Matter Searches, Doctoral thesis, Tsinghua, 2018
[8] Q. Hu, et al., NIMA, 859 (2017) 37–40
[9] Zhaoming Zeng, Research and Application of Low Background Thermal Neutron Detection Technology, Tsinghua, 2017
[10] Z. Zeng, et al., NIMA, 804 (2015) 108–112
[11] Q. Du, et al., NIMA, 889 (2018) 105–112
[12] Sato T, Expacs excel-based program for calculating atmospheric cosmic-ray spectrum, https://phits.jaea.go.jp/expacs/
[13] J. Su, et al., High Power Laser and Particle Beams, 2015, DOI:10.3788/HPLPB20122412.3015